A Comparative Analysis for Predicting Ship Squat in Shallow Water

Kazi Naimul Hoque[1*], Awlad Alam Mahmud[1]

[1]*Department of Naval Architecture and Marine Engineering, Bangladesh University of Engineering and Technology (BUET), BUET Central Road, Dhaka-1000, Bangladesh*

---***---

Abstract:

This paper focuses on predicting the sea-keeping characteristics of ships, with a specific emphasis on the "Squat Effect" when ships operate with limited underkeel clearance. The severity of this problem becomes more pronounced at higher speeds. The main objective of this investigation is to predict the squat phenomenon concerning different ship shapes and speeds. It has been observed that both sinkage and trim associated with the squat effect increase as the square of the ship's speed. To expedite the computation of ship squat using essential ship particulars, several reliable programs are developed based on various squat formulae. These programs serve as efficient tools for quickly estimating ship squat values. Moreover, the study compares the ship squat results obtained by different researchers, facilitating insights into the accuracy and reliability of various prediction methods. By consolidating and analyzing this collective knowledge, the paper aims to enhance the understanding of the squat effect and its implications for ships navigating with limited underkeel clearance at varying speeds.

Keywords*: Squat effect; ship speed; bow squat; block coefficient; boundary layer thickness; shear stress.*

NOMENCLATURE

L_{pp}	Length between perpendiculars	R_{LB}	Ratio of length of ship and breadth of ship
B	Breadth of ship	R_{hT}	Ratio between depth of water and depth of ship
D	Draught of ship	∇	Volumetric displacement of ship
T	Depth of ship	ρ	Density of fluid
h	Depth of channel	Re_x	Reynolds number
C_b	Block coefficient of ship	S_b	Bow squat
V_s	Velocity of the vessel in m/s	δ	Boundary layer thickness
V_k	Velocity of vessel in knots	τ	Shear stress
F_{nh}	Froude number, based on depth		

1. INTRODUCTION

In the ever-expanding shipping industry worldwide, achieving minimum voyage and port turnaround times has become a top priority for ship operations. However, as ships increase their speed, they encounter deteriorating sea-keeping characteristics caused by various motions and phenomena like heaving, pitching, yawing, and more. Another phenomenon which is often overlooked in the study of sea-keeping characteristics is the "Squat Effect".

The phenomenon of squats is typified by the alteration in a vessel's position, both in terms of sinkage and trim, brought about by its forward motion. When the ship propels ahead, it generates a relative speed disparity between itself and the encompassing water, culminating in an upsurge in dynamic pressure coupled with a subsequent decline in static pressure. This resultant velocity configuration gives rise to a modification in hydrodynamic pressure distribution along the vessel, reminiscent of the Bernoulli principle, where equilibrium between kinetic and potential energy is maintained. This dynamic manifests in a downward vertical force and a rotational effect around the lateral axis, leading to distinct magnitudes at the bow and stern sections.

The exploration of the phenomenon known as "Squat" within naval architecture traces its origins to the preceding century, and its significance has progressively heightened, particularly within the context of investigating high-speed occurrences and their pertinence to seafaring vessels, especially in shallower waterways. Most documented findings are rooted in empirical investigations.

A pivotal stride in comprehending "Squat" was taken by Tuck (1966), who embarked on an innovative study, employing matched asymptotic expansions to establish approximate solutions [1]. Through this endeavor, he derived equations for wave resistance, vertical forces, and pitching moments, encompassing both subcritical scenarios (where the depth Froude number is below 1.0) and supercritical circumstances (where the depth Froude number surpasses 1.0) for ship velocities. Tuck also laid the foundation for non-dimensional coefficients governing sinkage and trim, uncovering a noteworthy pattern: sinkage dominates in subcritical speeds, while trim takes precedence in supercritical velocities. His findings revealed a commendable concurrence with outcomes obtained from model experiments.

Building on the groundwork laid by Tuck, Beck et al. (1975) extended the scope of investigation to encompass channels that have been dredged, featuring shallower peripheral areas adjacent to the deeper central channel [2]. They engaged in solving boundary value predicaments to foresee variations in sinkage, trim, and ship resistance for ship speeds that are categorized as subcritical within the central channel, as well as subcritical or supercritical within the peripheral regions. Their conclusions brought to light a noteworthy revelation: the shallower peripheral sections exert a substantial influence on sinkage, trim, and wave resistance, a phenomenon particularly evident in confined waterways and at elevated ship speeds. This effect is especially pronounced when the depths of the peripheral areas surpass those of the interior channel. The study by Beck et al. (1975) demonstrated a strong correlation across an array of different vessel types [2].

PIANC (1997) released a compendium of empirical equations concerning squat effects, addressing a spectrum of ship and channel setups [3]. Within this array, the advisory inclination gravitated towards favoring the ICORELS (1980), Barrass (1979), and Eryuzlu et al. (1978, 1994) formulae, deemed to encapsulate typical squat outcomes [4-7]. Notably, Barrass (1981) proposed a bow squat formula, substantiating its accuracy through validation against measurements taken at full scale [8]. Furthermore, distinctive equations for both bow and stern squat were deduced by diverse researchers through rigorous physical model experiments, spanning all three channel configurations.

In a separate study, Demirbilek and Sargent (1999) brought forth a noteworthy observation, revealing substantial divergence among these assorted formulae [9]. Their analysis underscored that adopting the more cautious or pessimistic forecasts, those which anticipate larger squat magnitudes, might be prudent, especially when considering heightened risks of bottom contact.

2. SQUAT EFFECT

When a ship advances through water, it displaces water in front of it. To maintain a continuous flow of water, this displaced volume must return along the sides and beneath the ship. The relative velocity of this returning flow is slightly greater than the ship's speed, resulting in a decrease in static pressure, causing the ship to sink vertically into the water.

In addition to the vertical sinking, the ship typically trims forward or aft. The overall reduction in the static clearance under the keel, whether forward or aft, is known as “Ship Squat”. If a ship moves too quickly in shallow waters, where the static clearance under the keel is, for example, 1.0 to 1.5 meters, it could be grounded either at the bow or stern due to excessive squat. For full-form vessels like supertankers, grounding typically occurs at the bow. Conversely, for fine-form vessels like passenger liners or container ships, grounding usually happens at the stern, assuming they are on an even keel when not in motion. However, it's important to note that recent trends in ship design, with shorter length and wider breadth, have led to reported groundings near the midship bilge strakes during slight rolling motions.

Additionally, the boundary layer also plays a role in situations with limited under-keel clearance. For a ship with a length of around 300 meters, the boundary layer at the stern can extend 2 to 2.5 meters, potentially exceeding the available under-keel clearance in shallow channels. The interaction between the boundary layer and the channel bottom can affect the ship's operational behavior.

Overall, ship squats are a significant and potentially damaging phenomenon that primarily impacts the bow of a vessel, reducing propulsion efficiency, compromising performance, and causing the ship to sink deeper into the water.

3. BASIC FORMULATION

This paper focuses on investigating various empirical formulae proposed by numerous researchers for calculating squat values. Each formula is carefully studied, and subsequently, a dedicated program is developed using the FORTRAN 95 language. These programs are designed to compute the squat values for different ship speeds (V_k) and block coefficients (C_b). To facilitate the calculations, the following ship particulars are assumed:

Length between perpendiculars of the ship,
L_{pp} = 320 m
Breadth of the ship, B = 55 m
Draught of the ship, D = 13.5 m
Depth of water, h = 16 m

Each formula's computed values are presented in tabular form in this study. Additionally, graphical representations are provided, with squat (S_b) on the ordinate and ship speed (V_k) on the abscissa. Furthermore, a thorough comparison among the predicted values from different formulae is presented both in tabular and graphical formats, allowing for a comprehensive analysis of their performance.

The ICORELS (International Commission for the Reception of Large Ships) formula (1980) for bow squat S_b is defined as [4],

$$S_b = 2\cdot 4 \times \frac{\nabla}{L_{pp}^2} \times \frac{F_{nh}^2}{\sqrt{1-F_{nh}^2}} \qquad (1)$$

The PIANC (1997) noted that the “2.4” constant is sometimes replaced with a smaller value of “1.75” for full form ships with larger C_b [3].

Millward (1990) undertook a series of physical model experiments utilizing towed scale models, encompassing diverse vessel types, all in unrestricted channels characterized by widths roughly twice the vessel's length overall (L_{PP}) [10]. Millward’s derived formula likely embraces a cautious perspective, leaning towards safety by tending to forecast significant squat values [10]. Notably, his experiments were confined to a restricted range of ship lengths, limiting the applicability of his squat predictions to the newer and longer vessels. The expression for the maximum bow squat (S_b) from Millward's formulation is as follows [10],

$$S_b = 0\cdot 01 \times L_{PP} \times \left(15 \times C_b \times \frac{1}{L_{PP}/_B} - 0\cdot 55\right) \times \frac{F_{nh}^2}{1-0\cdot 9 \times F_{nh}} \qquad (2)$$

Millward (1992) rearranged his test results and presented them in a format [11]. The formula for bow squat is given by [11],

$$S_b = 0\cdot 01 \times L_{PP} \times \left(61\cdot 7 \times C_b \times \frac{1}{L_{PP}/_T} - 0\cdot 6\right) \times \frac{F_{nh}^2}{\sqrt{1-F_{nh}^2}} \qquad (3)$$

Norrbin (1986) developed a formula for bow squat S_b based on the work of Tuck and Taylor (1970) for a ship in an unrestricted channel [12]. His predictions satisfied the constraint that F_{nh} < 0.4 and is thus somewhat limited in its application. It is given by:

$$S_b = \frac{C_b}{15} \times \left(\frac{1}{L_{PP}/_B}\right) \times \left(\frac{1}{h/_T}\right) \times V_K^2 \qquad (4)$$

It is noted that two of the factors in the equation for S_b are equivalent to the standard non-dimensional ratios R_{LB} and R_{hT}.

The paramount non-dimensional factor is the depth Froude number, denoted as F_{nh}, signifying the vessel's resistance against movement in shallow waters. In practical terms, most ships possess inadequate power to surmount F_{nh} values surpassing 0.6 for tankers and 0.7 for container ships. A significant portion of empirical equations necessitates F_{nh} to remain below the threshold of 0.7. In all instances, it's imperative that the F_{nh} value adheres to F_{nh} < 1, representing a critical limit to effective speed. Mathematically, the dimensionless F_{nh} is formulated as follows:

$$F_{nh} = \frac{V_S}{\sqrt{gh}} \qquad (5)$$

The boundary layer thickness (δ) also seems to have an influence on ships motion. The general character of boundary layer may be estimated based on flat plate boundary layer theory. For a turbulent boundary layer past a flat plate, the boundary layer thickness δ grows downstream from the leading edge according to the approximate empirical relation:

$$\delta = \frac{0.16x}{\sqrt[7]{Re_x}} \qquad (6)$$

An empirical formulation for the wall shear stress, τ due to an unrestricted turbulent boundary layer flowing past a smooth flat plate i,

$$\tau = \rho V^2 \frac{0.014}{\sqrt[7]{Re_x}} \qquad (7)$$

4. RESULTS AND DISCUSSION

The provided figures offer a comprehensive insight into the effects of vessel speed and C_b on bow squat, boundary layer thickness, and shear stress. Figures 1(a) to 1(d) illustrate the variations in vessel's bow squat with ship speed for different C_b values ranging from 0.5 to 0.9. Similarly, Figures 2(a) to 2(d) provide a comparative analysis of bow squat across various formulae given by ICORELS (1980), Millward (1990), Millward (1992), and Norrbin (1986), encompassing C_b values from 0.6 to 0.9 [4, 10-12]. Furthermore, Figures 3 and Figure 4 depict the changes in boundary layer thickness (δ) and shear stress (τ) concerning distance from the vessel's leading edge (x) at different vessel speeds (V_k).

Figure 1(a) illustrates the variation of bow squat of a vessel, expressed in meters, as a function of the vessel's velocity in knots. This depiction encompasses a spectrum of C_b values, ranging from 0.5 to 0.9, as dictated by the formulation provided by ICORELS (1980) [4]. Across all instances, the ascent of bow squat exhibits a notably steep incline in conjunction with the augmentation of ship velocity. In the scenario of a C_b value of 0.5, the surge in bow squat is marginal, achieving a pinnacle of unity when the speed attains 14 knots. Conversely, with a C_b of 0.9, the magnitude of bow squat elevates to a peak of 2 m at the identical speed of 14 knots. The remaining curves are situated between these boundaries, aligning with C_b values of 0.5 and 0.9.

Figure 1(b) shows the variation of bow squat of a vessel in meters as a function of ship speed in knots for different values of C_b ranging from 0.5 to 0.9, according to the formulation given by Millward (1990) [10]. The curve shows that the bow squat increases significantly with the increase of ship speed. The maximum value of bow squat is around 4 m for C_b =0.9 and around 1.5 m for C_b =0.5 corresponding to a speed of 14 knots. The remaining curves fall between these two extreme curves for C_b =0.5 and C_b =0.9 in which the increase is gradual for all the cases.

Figure 1(c) illustrates the variation of bow squat of a vessel in meters, relative to ship speed in knots, for different C_b values varying from 0.5 to 0.9 based on Millward's (1992) formulation [11]. In contrast to the notable increase observed in Millward (1990), the curves here show a less dramatic growth in bow squat. The maximum bow squat value occurs at a speed of 14 knots, slightly exceeding 0.5 m for C_b = 0.5, and approximately 2 m for C_b = 0.9. The other curves fall within this range and share similar characteristics with the other depicted curves.

Figure 1(d) depicts the variability of vessel's bow squat in meters, plotted against ship speed in knots, across distinct C_b values ranging from 0.5 to 0.9 using the formula devised by Norrbin (1986) [12]. Unlike the steeper trends observed in other bow squat curves with increasing ship speed, the curves here exhibit a more gradual increase in bow squat. This formula, designed for ships in unrestricted channels, has limited applicability and is constrained by F_{nh} < 0.4. The peak bow squat occurs at a speed of 9 knots, amounting to 0.7 m for C_b =0.9 and approximately 0.4 m for C_b =0.5. The remaining curves fall within the range defined by these two extreme curves.

Figure 2(a) represents the comparison of bow squat (for C_b =0.6) in meters against ship speed in knots among various formulae developed by ICORELS (1980), Millward (1990), Millward (1992) and Norrbin (1986) [4, 10-12]. All the curves for bow squat increase rapidly with the rise of ship speed. The curve for Millward (1990) is sharper than the other curves giving a maximum value of just above 2 m, while the curve for Millward (1992) shows a slight increase in bow squat having a maximum value of just above 1 m for the corresponding speed of 14 knots. This means that the effect of bow squat is more significant in case of former one than the latter. The other two curves for ICORELS (1980) and Norrbin (1986) coincide with each other in which ICORELS (1980) extends up to 14 knots giving a peak value of just under 1.5 m while the curve for Norrbin (1986) cannot extend beyond 9 knots due to the limitations and F_{nh} < 0.4, giving a peak value of around 0.5 m at those speed. The effect of bow squat is less significant for these two curves.

Figure 2(b) provides a comparison of bow squat (for C_b = 0.7) in meters against ship speed in knots, considering formulae developed by ICORELS (1980), Millward (1990), Millward (1992), and Norrbin (1986) [4, 10-12]. All the bow squat curves demonstrate a pronounced increase with increasing ship speed. Notably, the curve corresponding to Millward (1990) displays a steeper increase, reaching a peak value just below 3 m at 14 knots, signifying a more impactful bow squat effect. The remaining three curves for ICORELS (1980), Millward (1992), and Norrbin (1986) closely align, yielding a peak value of about 1.5 m at a speed of 14 knots. However, the curve for Norrbin (1986) is limited by its applicability and cannot extend beyond 9 knots due to F_{nh} < 0.4 constraints, resulting in a peak value of 0.5 m. The effect of bow squat is less pronounced for these latter curves in contrast to the more prominent impact observed with Millward (1990).

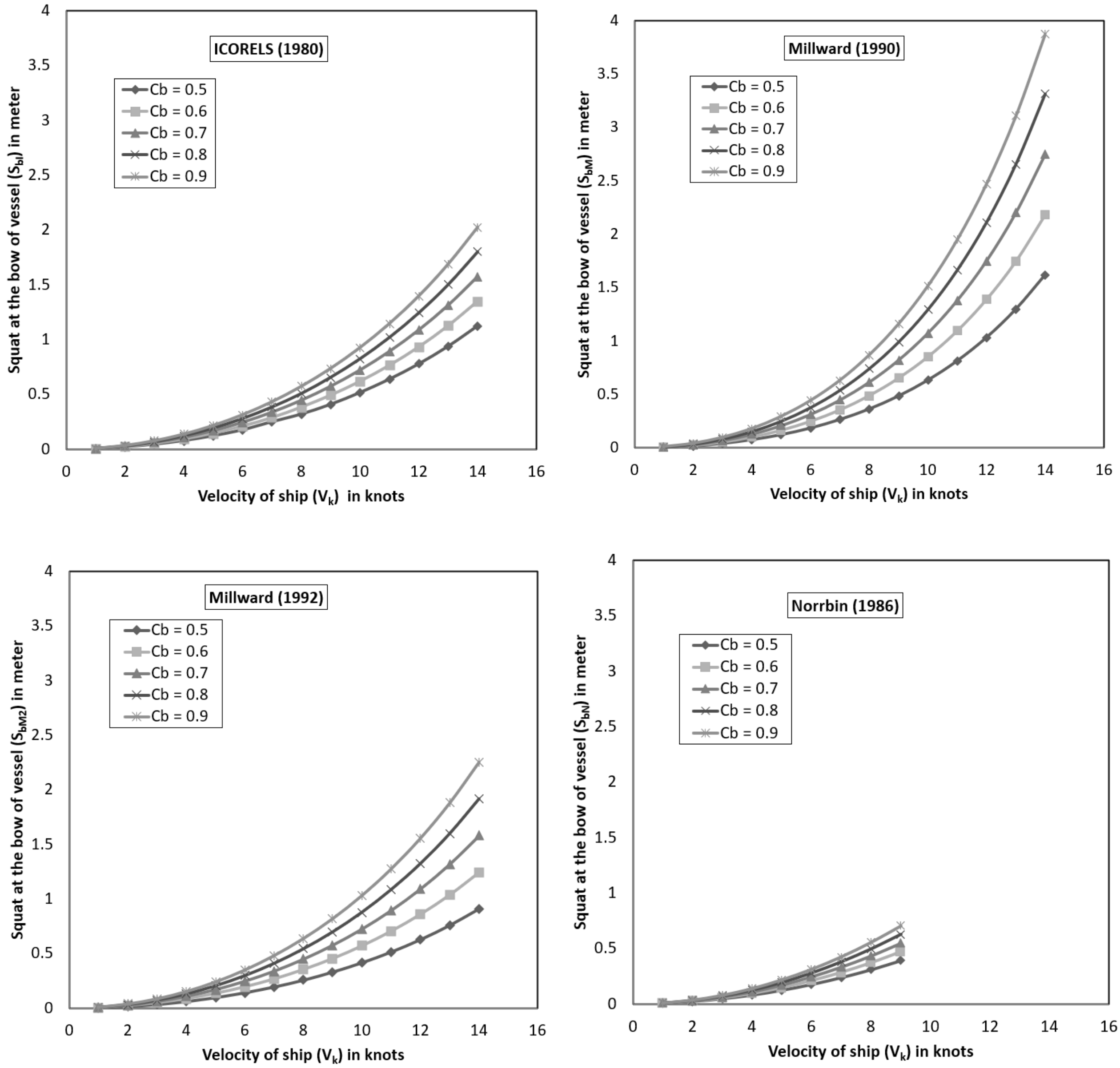

Figure 1. Variation of bow squat (S_b) with velocity of ship (V_k) for different C_b by (a) ICORELS (1980), (b) Millward (1990), (c) Millward (1992), and (d) Norrbin (1986).

Figure 2(c) displays a comparative analysis of bow squat (for C_b = 0.8) in meters against ship speed in knots, encompassing multiple formulations including ICORELS (1980), Millward (1990), Millward (1992), and Norrbin (1986) [4, 10-12]. All the bow squat curves exhibit a notable increase with the increase of ship speed. The curve representing Millward (1990) displays a more pronounced incline, reaching a peak value of approximately 3.5 m at 14 knots, underscoring its significant impact. In contrast, the curve for Millward (1992) shows a less steep incline, giving a maximum value of about 2 m. This highlights the greater significance of the bow squat effect in the former formula compared to the latter. The remaining two curves, ICORELS (1980) and Norrbin (1986), coincide, with ICORELS' (1980) peak value just above 1.5 m at a speed of 14 knots. On the other hand, Norrbin (1986) reaches a peak value of around 0.5 m at a speed of 9 knots, reflecting its limited applicability. These two curves offer more reliable values for mitigating the squat effect.

Table 1: Variation of S_b with V_k for different C_b by ICORELS (1980).

Velocity of Ship (knots)	C_b = 0.5	C_b = 0.6	C_b = 0.7	C_b = 0.8	C_b = 0.9
	bow squat (meter)	bow squat (meter)	bow squat (meter)	bow squat (meter)	bow squat (meter)
1	0.005	0.006	0.007	0.008	0.008
2	0.019	0.023	0.026	0.03	0.034
3	0.043	0.051	0.06	0.068	0.077
4	0.076	0.091	0.107	0.122	0.137
5	0.12	0.144	0.168	0.192	0.216
6	0.174	0.209	0.244	0.279	0.314
7	0.248	0.286	0.336	0.384	0.432
8	0.318	0.382	0.445	0.507	0.573
9	0.407	0.491	0.573	0.655	0.737
10	0.515	0.618	0.721	0.824	0.927
11	0.637	0.764	0.891	1.019	1.146
12	0.777	0.932	1.087	1.243	1.398
13	0.938	1.126	1.313	1.501	1.689
14	1.124	1.349	1.574	1.799	2.024

Table 2: Variation of S_b with V_k for different C_b by Millward (1990).

Velocity of Ship (knots)	C_b = 0.5	C_b = 0.6	C_b = 0.7	C_b = 0.8	C_b = 0.9
	bow squat (meter)	bow squat (meter)	bow squat (meter)	bow squat (meter)	bow squat (meter)
1	0.004	0.006	0.007	0.008	0.01
2	0.017	0.023	0.029	0.035	0.041
3	0.04	0.054	0.069	0.083	0.097
4	0.075	0.101	0.127	0.153	0.179
5	0.122	0.165	0.208	0.25	0.293
6	0.184	0.249	0.313	0.377	0.442
7	0.264	0.355	0.447	0.539	0.631
8	0.362	0.489	0.615	0.741	0.868
9	0.484	0.653	0.821	0.99	1.159
10	0.632	0.853	1.074	1.294	1.515
11	0.813	1.096	1.38	1.663	1.947
12	1.032	1.391	1.751	2.111	2.471
13	1.297	1.747	2.201	2.654	3.106
14	1.619	2.184	2.749	3.313	3.875

Table 3: Variation of S_b with V_k for different C_b by Millward (1992).

Velocity of Ship (knots)	C_b = 0.5	C_b = 0.6	C_b = 0.7	C_b = 0.8	C_b = 0.9
	bow squat (meter)	bow squat (meter)	bow squat (meter)	bow squat (meter)	bow squat (meter)
1	0.004	0.005	0.007	0.008	0.009
2	0.015	0.021	0.026	0.032	0.038
3	0.034	0.047	0.06	0.073	0.085
4	0.061	0.084	0.107	0.13	0.152
5	0.097	0.133	0.168	0.204	0.24
6	0.141	0.193	0.245	0.297	0.349
7	0.194	0.265	0.337	0.409	0.481
8	0.256	0.352	0.447	0.542	0.637
9	0.33	0.452	0.575	0.697	0.819
10	0.415	0.569	0.723	0.877	1.031
11	0.513	0.704	0.894	1.085	1.275
12	0.626	0.859	1.091	1.323	1.556
13	0.756	1.037	1.318	1.598	1.879
14	0.906	1.243	1.579	1.915	2.252

Table 4: Variation of S_b with V_k for different C_b by Norrbin (1986).

Velocity of Ship (knots)	C_b = 0.5	C_b = 0.6	C_b = 0.7	C_b = 0.8	C_b = 0.9
	bow squat (meter)	bow squat (meter)	bow squat (meter)	bow squat (meter)	bow squat (meter)
1	0.005	0.006	0.007	0.008	0.009
2	0.019	0.023	0.027	0.031	0.035
3	0.044	0.052	0.061	0.07	0.078
4	0.077	0.093	0.108	0.124	0.139
5	0.121	0.145	0.169	0.193	0.218
6	0.174	0.209	0.244	0.278	0.313
7	0.237	0.284	0.332	0.379	0.426
8	0.309	0.371	0.433	0.495	0.557
9	0.392	0.47	0.548	0.626	0.705

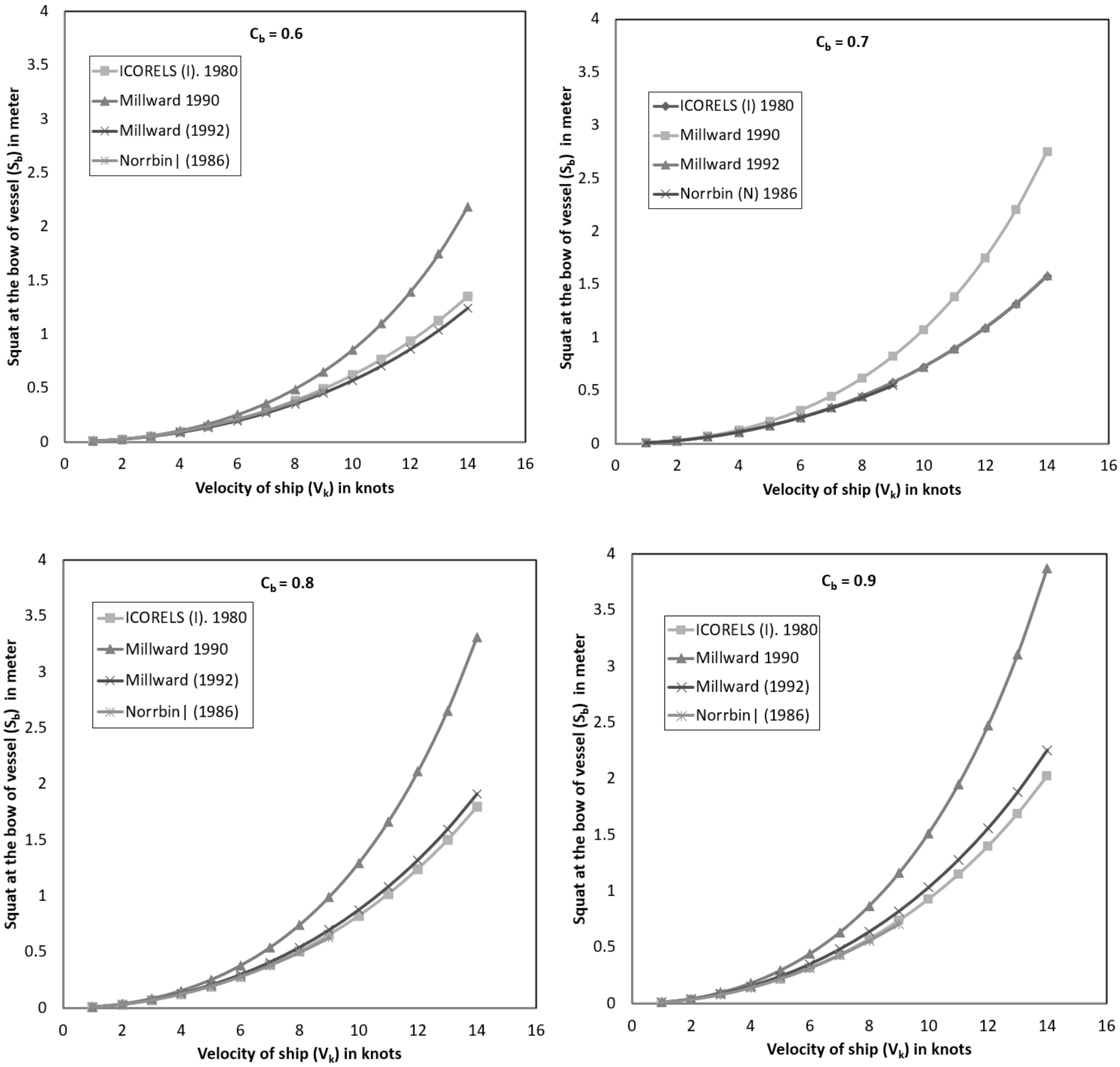

Figure 2. Comparison of bow squat (S_b) for different velocity of vessel (V_k) among various formulae developed by ICORELS (1980), Millward (1990), Millward (1992) and Norrbin (1986) at (a) C_b = 0.6, (b) C_b = 0.7, (c) C_b = 0.8, and (d) C_b = 0.9.

Figure 2(d) represents the comparison of bow squat (for C_b =0.9) in meters against ship speed in knots among various formulae developed by ICORELS (1980), Millward (1990), Millward (1992) and Norrbin (1986) [4, 10-12]. For all these curves, bow squat increases sharply with the rise of ship speed. The curve for Millward (1990) is sharper than the other curves, giving a maximum value of bow squat of around 4 m at a speed of 14 knots. The curve for Millward (1992) is less sharp than the previous one, giving a peak value of around 2 m. So, the curve for Millward (1992) is more reliable in comparison with Millward (1990) in minimizing the effect of bow squat. The remaining two curves corresponding to ICORELS (1980) and Norrbin (1986) align closely, presenting a peak value of 2 m at a speed of 14 knots for ICORELS (1980). However, the curve associated with Norrbin (1986) is constrained by its applicability and cannot extend beyond a speed of 9 knots due to limitations tied to F_{nh} < 0.4. Consequently, it yields a peak value of around 0.7 m at these speeds. The bow squat effect depicted by these curves is comparatively less pronounced when contrasted with the curves outlined by Millward (1992) and Millward (1990).

Figure 1 (a to d) and Figure 2 (a to d) explore how vessel speed and C_b influence bow squat. As ship speed increases, bow squat exhibits a steep rise across all scenarios. Notably, higher C_b values lead to increased bow squat, reaching peaks at 2 m (C_b = 0.9). Formulations by Millward (1990) and Millward (1992) demonstrate significant increases in bow squat, while Norrbin's formula (1986) yields more subdued results. Millward (1992) proves to be a reliable means of mitigating bow squat's effects. The corresponding values of bow squat with ship speed at different C_b values, developed by ICORELS (1980), Millward (1990), Millward (1992), and Norrbin (1986), are detailed in Table 1 to Table 4.

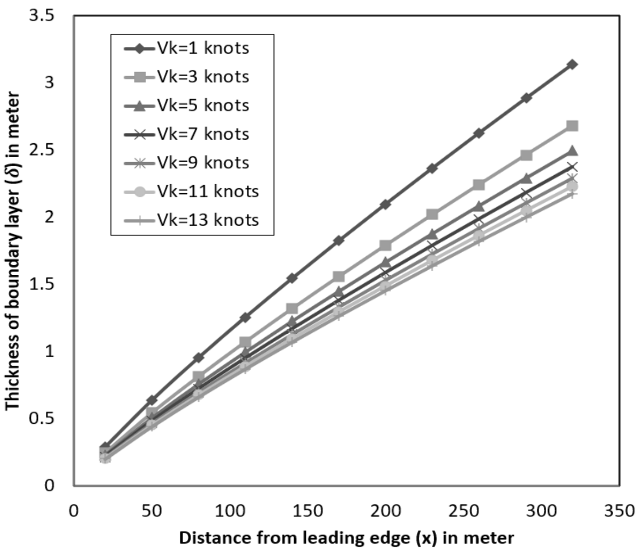

Figure 3. Variation of boundary layer thickness (δ) as function of distance from the leading edge of vessel (x) for different values of velocity of the vessel (V_k).

Figure 3 presents a graphical representation illustrating the dynamic alterations in boundary layer thickness (δ) concerning its relationship with the distance measured from the leading edge of the vessel (x). This visualization encompasses a spectrum of distinct velocity values for the vessel (V_k). Evidently, the boundary layer thickness experiences a progressive augmentation as the measurement distance from the vessel's leading-edge increases. Of noteworthy significance is the observation that the most substantial magnitude of boundary layer thickness for any designated distance emerges when the vessel is operating at its lowest speed. Intriguingly, this maximum thickness value diminishes as the vessel's speed increases. In essence, there exists an inverse correlation between the vessel's speed and the magnitude of its boundary layer thickness, as demonstrated by the trends depicted in the graph.

Figure 3 showcases the dynamic relationship between boundary layer thickness (δ) and the distance from the vessel's leading edge (x) at varying velocities (V_k). A consistent pattern emerges as x increases, δ also grows. The maximum thickness occurs at the lowest vessel speed, decreasing as speed rises. This reveals an inverse correlation between vessel speed and boundary layer thickness. The variation of boundary layer thickness (δ) with respect to distance from the leading edge of vessel (x) for different values of V_k are detailed in Table 5.

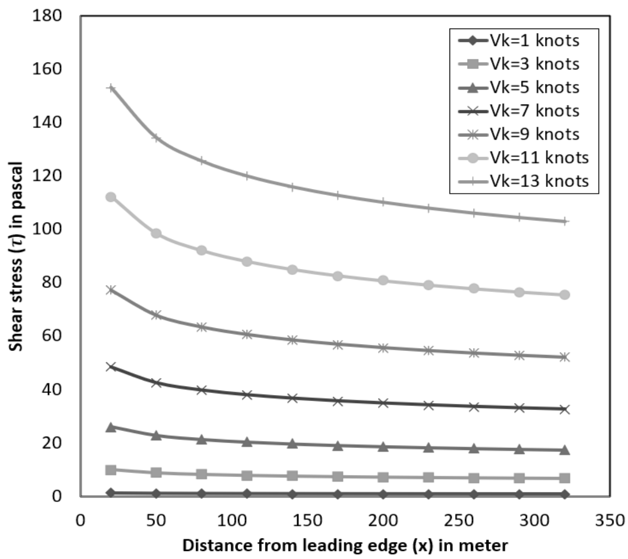

Figure 4. Variation of Shear stress (τ) as function of distance from the leading edge of vessel (x) for different values of velocity of the vessel (V_k).

Figure 4 provides an illustrative presentation highlighting the nuanced changes in shear stress (τ) concerning its interplay with the distance traversed from the leading edge of the vessel (x). This depiction encompasses a spectrum of diverse velocity values attributed to the vessel (V_k). Evidently, a discernible pattern emerges: the shear stress experiences a progressive attenuation as one moves away from the vessel's leading edge. A pivotal observation of note is the marked occurrence of the highest shear stress value when the vessel is operating at its peak speed. This maximum value surfaces when the vessel is at its utmost velocity. Particularly noteworthy is the revelation that the rate of this decrease in shear stress is particularly prominent when the vessel is moving at higher velocities, especially in proximity to the leading edge (represented by smaller x values). This emphasizes that the attenuation of shear stress is more pronounced when the vessel's speed is greater. Conversely, at lower velocities, the shear stress values tend to be of trivial significance. This discrepancy in shear stress magnitude between low and high velocities signifies the complex interplay between vessel speed and the resultant shear stress, which is acutely dependent on the vessel's position relative to its leading edge.

Table 5: Variation of boundary layer thickness (δ) as function of distance from the leading edge of vessel (x) for different values of V_k.

Distance from leading edge (meter)	boundary layer thickness for V_k = 1 knots	boundary layer thickness for V_k = 3 knots	boundary layer thickness for V_k = 5 knots	boundary layer thickness for V_k = 7 knots	boundary layer thickness for V_k = 9 knots	boundary layer thickness for V_k = 11 knots	boundary layer thickness for V_k = 13 knots
20	0.291	0.249	0.232	0.221	0.213	0.207	0.202
50	0.639	0.546	0.508	0.484	0.467	0.454	0.443
80	0.956	0.817	0.76	0.724	0.699	0.679	0.663
110	1.257	1.074	0.998	0.952	0.918	0.892	0.871
140	1.545	1.321	1.228	1.17	1.129	1.097	1.071
170	1.825	1.56	1.45	1.382	1.333	1.296	1.265
200	2.098	1.793	1.667	1.589	1.533	1.489	1.454
230	2.365	2.021	1.879	1.791	1.728	1.679	1.639
260	2.627	2.245	2.087	1.989	1.919	1.865	1.821
290	2.884	2.465	2.292	2.184	2.107	2.048	1.999
320	3.138	2.682	2.494	2.377	2.293	2.228	2.175

Table 6: Variation of shear stress (τ) as function of distance from the leading edge of vessel (x) for different values of V_k.

Distance from leading edge (meter)	shear stress in (Pa) for V_k = 1 knots	shear stress in (Pa) for V_k = 3 knots	shear stress in (Pa) for V_k = 5 knots	shear stress in (Pa) for V_k = 7 knots	shear stress in (Pa) for V_k = 9 knots	shear stress in (Pa) for V_k = 11 knots	shear stress in (Pa) for V_k = 13 knots
20	1.307	10.055	25.964	48.501	77.347	112.278	153.12
50	1.147	8.821	22.778	42.55	67.857	98.503	134.333
80	1.072	8.248	21.299	39.787	63.451	92.106	125.61
110	1.025	7.881	20.352	38.017	60.629	88.01	120.024
140	0.99	7.614	19.663	36.73	58.576	85.029	115.959
170	0.963	7.406	19.125	35.725	56.973	82.703	112.787
200	0.941	7.236	18.686	34.905	55.666	80.805	110.199
230	0.922	7.093	18.316	34.215	54.565	79.208	108.02
260	0.906	6.97	17.998	33.621	53.618	77.833	106.145
290	0.892	6.862	17.72	33.101	52.788	76.628	104.502
320	0.88	6.766	17.472	32.639	52.051	75.558	103.042

Figure 4 elucidates the intricate interplay between shear stress (τ) and distance from the vessel's leading edge (x), considering different V_k values. Notably, shear stress declines progressively as x increases. The highest shear stress occurs at the peak vessel speed, especially in proximity to the leading edge. At high velocities, shear stress attenuation is more pronounced. Conversely, lower velocities yield lower shear stress values. This underlines the complex relationship between vessel speed and shear stress, dependent on the vessel's position relative to its leading edge. The relationship between shear stress (τ) and the distance from the leading edge of the vessel (x) is detailed in Table 6 for various V_k values.

In summary, the combined information presented in the Figures and Tables underscores the substantial influence of vessel velocity and block coefficient on bow squat, boundary layer thickness, and shear stress. These parameters play pivotal roles in the realm of ship hydrodynamics.

5. CONCLUSIONS

The key findings from this research can be summarized as follows:

- Bow squat:
  - Bow squat increases significantly with higher vessel speeds across all C_b values.
  - Higher C_b values lead to greater bow squat, with peak values observed at C_b = 0.9.
  - Formulations by Millward (1990) and Millward (1992) show more pronounced increases in bow squat compared to ICORELS (1980) and Norrbin (1986).
  - Millward (1992) appears to be a reliable formula for mitigating the bow squat effect.

- Boundary layer thickness:
  - Boundary layer thickness increases with distance from the vessel's leading edge.
  - The highest boundary layer thickness occurs at lower vessel speeds and decreases as speed increases.
  - There is an inverse correlation between vessel speed and boundary layer thickness.

- Shear stress:
  - Shear stress decreases as one moves away from the vessel's leading edge.
  - The highest shear stress values are observed at the highest vessel speeds, especially near the leading edge.
  - Shear stress attenuation is more pronounced at higher speeds.

Overall, these findings highlight the complex interplay between vessel speed, block coefficient, and their effects on bow squat, boundary layer thickness, and shear stress in ship hydrodynamics. Understanding these relationships is crucial for optimizing vessel design and navigation in various maritime conditions.

ACKNOWLEDGEMENT

The authors extend their heartfelt appreciation to all individuals who have offered invaluable assistance, both in direct and indirect capacities, across the diverse stages of this research endeavor. Additionally, the authors wish to convey their gratitude to the Department of Naval Architecture and Marine Engineering (NAME) at BUET, not only for granting access to the Journal Library but also for providing with a selection of highly beneficial papers that aided to this work significantly.

REFERENCES

[1] Tuck, E. O. (1966), Shallow-water flows past slender bodies, JFM, vol.26, no. 1, pp.81-95.
[2] Beck, R. F., Newman, J. N., and Tuck, E. O. (1975), Hydrodynamic forces on ships in dredged channels, J. Ship Research, vol. 19, no. 3, pp.166-171.
[3] PIANC. (1997), Approach channels: A Guide for design. Final Report of the Joint PIANC-IAPH Working Group II-30 in cooperation with IMPA and IALA, Supplement to Bulletin No. 95, June.
[4] ICORELS (International Commission for the Reception of Large Ships). (1980) Report on Working Group IV, PIANC Bulletin No. 35, Supplement.
[5] Barrass, C. B. (1979), The phenomenon of ship squat, International Shipbuilding Progress, vol. 26, pp. 44-47.
[6] Eryuzlu, N. E., and Hausser, R. (1978), Experimental investigation into some aspects of large vessel navigation in restricted waterways. Proceedings of the Symposium of Aspects of Navigability of Constraint Waterways Including Harbor Entrances, vol. 2, pp. 1-15.
[7] Eryuzlu, N. E., Cao, Y. L., and D'Agnolo, F. (1994), Underkeel requirements for large vessels in shallow waterways. 28t International Navigation Congress, PIANC, Paper S11-2, Sevilla, pp. 17-25.
[8] Barrass, C. B. (1981), Ship squat – A reply. The Naval Architect, pp. 268-272.
[9] Demirbilek, Z., and Sargent, F. (1999), Deep-draft coastal navigation entrance channel practice, Coastal

and Hydraulic Engineering Technical Note, pp. 1-11, March.
[10] Millward, A. (1990), A preliminary design method for the prediction of squat in shallow water. Marine Technology, vol. 27, no. 1, pp.10-19.
[11] Millward, A. (1992), A comparison of the theoretical and empirical prediction of squat in shallow water, International Shipbuilding Progress, vol.39, no.417, pp. 69-78.
[12] Norrbin, N. H. (1986), Fairway design with respect to ship dynamics and operational requirements, SSPA Research Report No. 102. Gothenburg, Sweden: SSPA Maritime Consulting.